SILVACO simulations of a monolithic active pixel sensor for low energy X-rays detection

Alessio Durante

Fermilab National Accelerator Laboratory

Politecnico di Milano
Electrical Engineering

adurante@fnal.gov
alessio.durante@mail.polimi.it

September 29, 2017

Abstract

In this report I present the work I performed during my stay at Fermilab for a summer internship program during August-September 2017. I will show my studies and results regarding TCAD simulations of an innovative monolithic active pixel sensor used for detecting low energy X-rays in imaging experiments at LCLS-II.

The structure of this paper is composed as follows:

- *PART 1 introduces the experiment LCLS-II and the general ideas behind the realisation of the new FLORA pixel sensor; after that an overview of the SILVACO software used for TCAD simulations is given.*

- *PART 2 shows the results of basic simulations about charge collection and transfer. Different solutions have been adopted and discussed.*

- *PART 3 shows the results of the simulations of the complete FLORA PIXEL sensor, the solutions adopted and some suggestions for the further developement.*

Not always the simulations have been run with the same temporal order reported here. The structure chosen is just thought for the maximum clarity and coherence.

As general result of all these analyses, a working version of the FLORA PIXEL comes out.
From the simulations done, I get errors down to 5%; it represents really a good result, given the accuracy of the simulations, the complexity of the sensor and the nature of the phenomena involved in its operation.
However there are still many pending issues which need a further developement.
With my work I hope to give useful guidelines and hints for the final realization of the sensor.

I'm looking forward for the realisation and testing of the sensor.

Contents

I INTRODUCTION **7**

1 The FLORA pixel **8**
1.1 Introduction . . . 8
1.2 Proposed structure . . . 9

2 SILVACO: TCAD simulations **10**

II ANALYSIS OF CHARGE COLLECTION AND TRANSFER **12**

3 Charge generation: photodiode **12**

4 Charge transfer from BSI to FD **14**
4.1 Single gate charge transfer . . . 14
4.1.1 First structure . . . 14
4.1.2 Study of the potential profile during the charge transfer . . . 16
4.1.3 Resetting the FD electrode . . . 17
4.2 Charge transfer with BSI gate . . . 19
4.2.1 TCAD simulation . . . 19
4.2.2 Charge collection verification . . . 22
4.3 Charge transfer with a J-FET structure . . . 23
4.3.1 Proposed structure . . . 23
4.3.2 Study of the potential needed to close the channel . . . 23
4.4 Pinned diode experiment . . . 25

III FLORA PIXEL **27**

5 Introduction of the overflow electrode **27**

6 Charge transfer with a BSI gate **28**
6.1 Structure . . . 28
6.2 Device TCAD simulation . . . 28

7 FLORA PIXEL: final version with pinned photodiode **32**
7.1 Structure and device simulation . . . 32
7.2 Device simulation: small signals . . . 32
7.3 Device simulation: large signals, overflow electrode . . . 35
7.3.1 BSI charge capacity . . . 36
7.4 Collection error . . . 37

8 Conclusions **38**

Part I
INTRODUCTION

In this report I will explain the results of my work of 2 months at Fermilab regarding TCAD simulations of an innovative monolithic active pixel sensor used for detecting low energy X-rays in imaging experiments at LCLS-II.

LCLS-II will be the world's only X-ray free-electron laser capable of supplying a uniformly-spaced train of pulses with programmable repetition rate with the highest speed and brightness ever realized (up to 1 million pulses per second).

Electrons will be accelerated through superconducting RF cavities, and they will emit X-rays thanks to undulator magnets.
LCLS-II will produce waves with coherent phase, good for sampling matter and taking picture at the atomic levels: it allows advanced research in chemistry, materials, biology and science of materials.

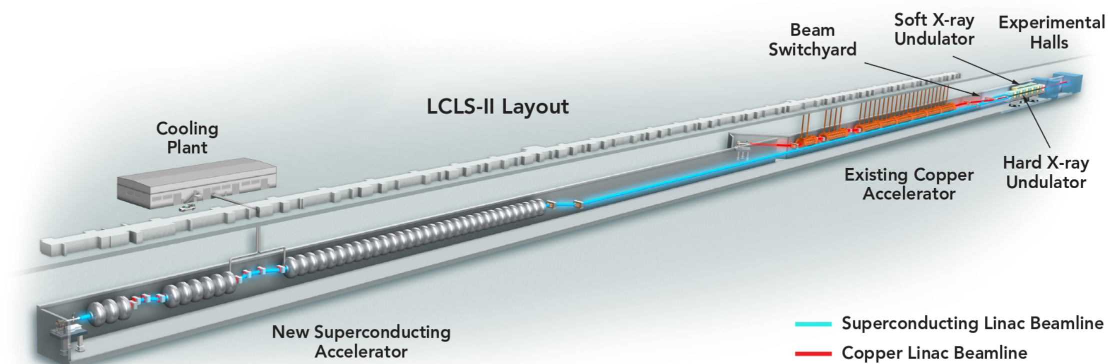

Figure 1: *LCLS-II*

X-rays' frequency ranges between 30 petahertz ($3 \cdot 10^{16}$ Hz) to 30 esahertz ($3 \cdot 10^{19}$ Hz). Hence their wavelength ranges from 0.01 to $10nm$. The spacing between atoms is of the order of nm (e.g. $C - C \approx 0.341$ nm).

The sample to be studied will be hit by the X-ray laser beam coming from LCLS-II. A detector is needed in order to measure the X-rays resulting from the diffraction phenomena occurring inside the sample.

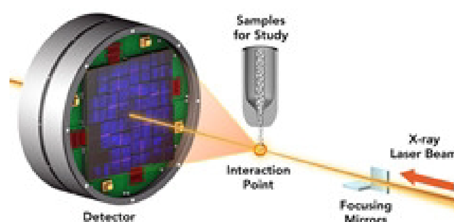

Figure 2: *Imaging experiment at LCLS-II*

Till now traditional monolithic active pixel sensors (MAPS) have been used as detectors for these kinds of experiments.
In this paper a new proposal for a detector is analyzed: the FLORA pixel.

1 The FLORA pixel

1.1 Introduction

The FLORA (**F**ermilab-**L**CLS CM**O**S 3D-integ**R**ated detector with **A**utogain) pixel is the new detector proposal for LSLS-II.

Traditionally monolithic active pixel sensors (MAPS) have always been used for detecting low signals due to their really high signal to noise ratio (SNR).

- *Monolithic*: both the electronics for charge collection and for the signal readout is included in the same silicon bulk;
- *Active*: the readout signal is amplified.

In these cases a source follower which is already included in the silicon has the task to process and amplify the output signal.

The innovation given by the FLORA pixel is providing two different paths for large and small signals.

Small signals will we collected and processes as it is done in a traditional monolithic active pixel sensor, which has a very high sensitivity and guarantees a very low noise. Conversely, large signals will flow through an overflow electrode with a lower sensitivity, after which they will be measured thanks to an external readout integrated circuit (ROIC).

Thanks to this idea, the FLORA pixel is thought to achieve very high dynamic range and signal to noise ratio. In particular, the foreseen targets are:

- *Dynamic range*: up to 10^4 photons;
- *Single photon detection*: with an energy in the range 200 $eV - 2\ keV$.

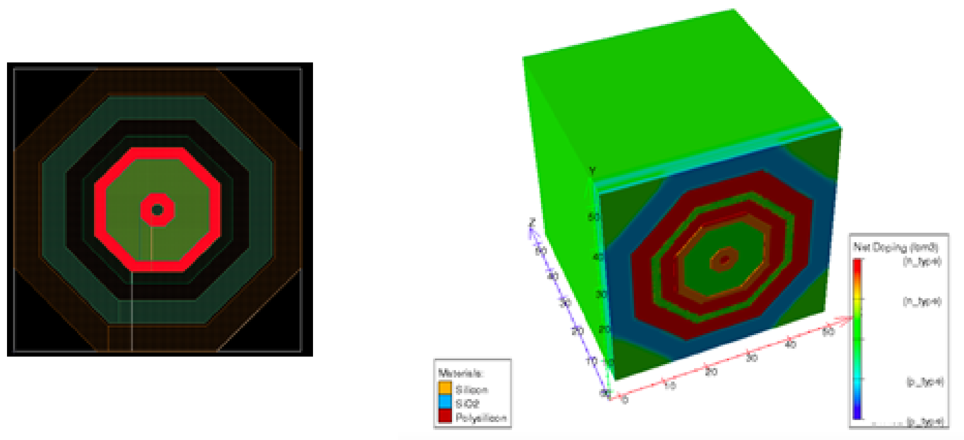

Figure 3: *FLORA pixel proposal*

The project is a collaboration between Fermilab and SLAC National Accelerator Laboratory, a U.S. laboratory operated by Stanford University.

TCAD simulations are required to test the operation of the pixel and to look for its optimization.

1.2 Proposed structure

The following structure is the initial proposal for the FLORA pixel. The structure is thought to be circular. In the figure a cross section along the diameter is represented. The yellow and orange regions are n-doped, while the blue regions are p-doped.

Figure 4: *Initial proposal for the FLORA pixel structure*

The substrate is n-doped. The p layer in the back creates the junction of the photo-diode. The junction is fully depleted.
Generated charges from an hitting X-ray are collected in the back side illuminated (BSI) photo-diode (PD), thanks to the p barriers which prevent charges to go elsewhere. In the sides of the structure the overflow electrodes guarantee a continuous charge flow through them in case that a very large quantity of charge is generated.
Conversely, small amounts of charges are collected in the BSI region and further transferred to the central floating diffusion region (n-doped) thanks to the transfer gates (H_G), in order to be measured with an high sensitivity.

The measure of the charge flowing through the overflow electrode (O_S) is performed by charging a big capacitor connected to the virtual ground provided by an operational amplifier (integrator circuit). Hence the overflow electrode is continuously at a fixed and constant potential. All this electronics will be in a ROIC constituted by an additional layer placed over the monolithic pixel.

The high precision measurement of small signals is performed by looking at the change in voltage of the floating diffusion (FD) region before and after charges have been deposited there. Since the capacitance of the FD region is very small, a little amount of charge produces a significant variation in potential, allowing a very sensitive measurement. This will be done by connecting a source follower to the FD electrode (H_S), which is integrated in the silicon structure. Notice that for this reason the FD electrode is always floating during the operation of the pixel.

The pixel is said to have an *autogain* because charges will flow automatically through the overflow electrode after they reach in amount a given threshold, regulated by the voltage to be applied on the overflow gates (O_G).

The p well on the topsides of the structures are fixed at a constant potential, as well as the p layer in the back.

2 SILVACO: TCAD simulations

SILVACO is a software which performs TCAD simulations of semiconductor devices.

TCAD allows fabrication process and device physics level simulations.

SILVACO

Figure 5: *SILVACO logo*

SILVACO exploits the 2D/3D Finite Element Method (FEM).

It performs the resolution of the semiconductor drift-diffusion (DD) equation and the Poisson's equation for the electric field over the mesh grid in the semiconductor structure. In includes many models of generation-recombination mechanisms, such as Shockley-Reed-Hall (SRH) for deep trap dynamics.

- ATHENA for process simulation;
- ATLAS for device simulation.

Here a diode, a p-MOS and a CMOS inverter simulated with SILVACO are shown, together with their static characteristics.

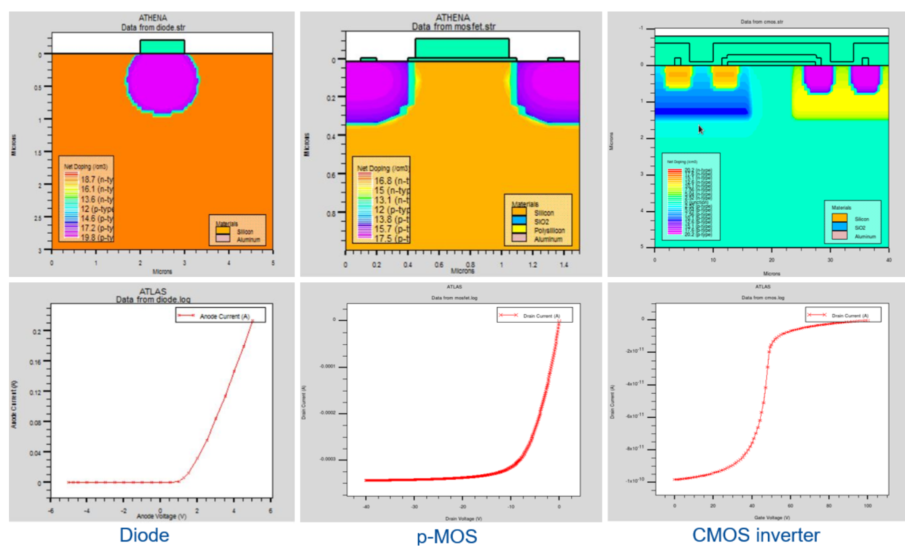

Figure 6: *SILVACO allows process and device simulations of semiconductor devices*

During simulations it's really important dealing with convergence problems: mesh and signals shape optimization are always needed.

Part II
ANALYSIS OF CHARGE COLLECTION AND TRANSFER

In this part basic simulations about semiconductor devices which allow charge collection and transfer are performed.
Moreover different solutions and proposals are deeply discussed.
The knowledge coming from these analyses allowed to put the right bricks together and paved the pay to the final proposal of the FLORA PIXEL sensor which will be developed in detail in section 7.

3 Charge generation: photodiode

A photodiode is a p-n junction which is always operated in reverse biased conditions. An external reverse field is used to extend the depletion region all along the depth of the structure. The conduction band is empty, i.e. almost no free charge carriers are present in the semiconductor structure. Fixed charges (positive charges in an n-doped region, negative charges in a p-doped region) create an approximately constant drift field in the depletion region.

A radiation hitting the silicon surface generates electron-hole pairs, breaking the bonds between electrons and nuclei. These free charges will drift according to the constant field in the depletion region of the p-n junction and will be collected at the electrodes.

The photodiode simulation is used to test the charge generation inside the silicon, as model for an hitting radiation on the illuminated surface of the detector.

In the following figure the structure of the photodiode is shown.

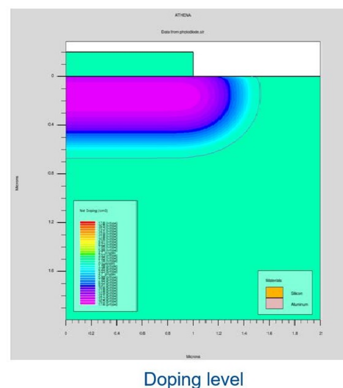

Figure 7: *Photodiode structure*

In the simulation, 0 V are applied to the anode (electrode at the p-doped region) and 5 V to the cathode (electrode at the n-doped region).

At time $t = 0$ charge is generated using the SingleEventUpset model and then it is collected at the electrode. In figure 8 the potential distribution, the electrons' concentration at the moment of the charge generations and the holes collected at the cathode are shown[1].
Electrons are collected at the anode analogously (not shown).

[1]Charge in SILVACO is conventionally positive if exiting from the silicon structure

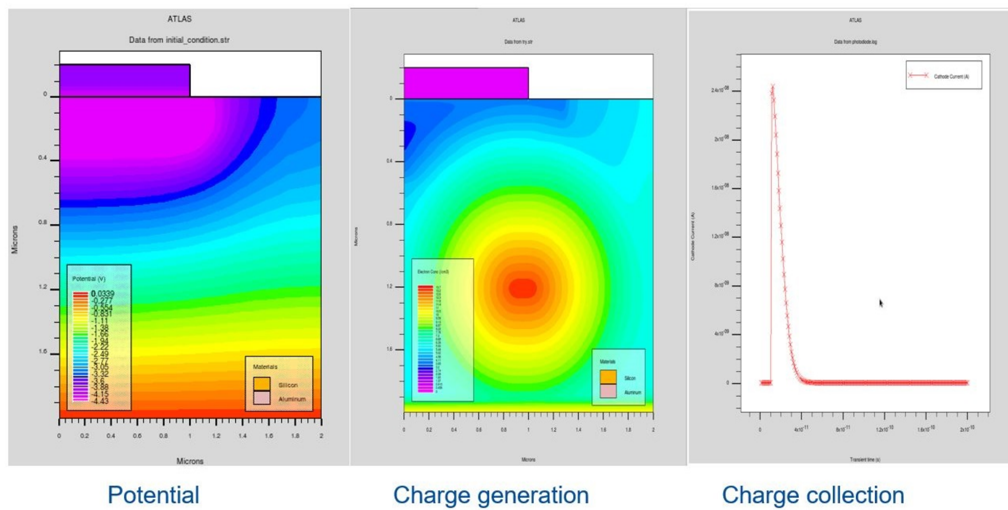

Figure 8: *Device simulation of the photodiode*

In this device, once the charge is generated, it will immediately drift according to the electric field.

In order to have the FLORA pixel working as desired, the possibility to collect charge in the silicon and then transfer them to the electrode when needed is necessary.
This operation will be the one which will allow to discriminate between low and large X-ray signals. Charges coming from low energy X-rays will be collected in a floating region in the silicon, while high amounts of charges coming from high energy X-rays will flow continuously in through an overflow electrode, as it happens in this photodiode.

In the next sections, in reference to the operation of the sensor in case of low signals, simulations about charge collection and transfer are performed and analyzed.

4 Charge transfer from BSI to FD

In this section, a possible structure which allows charge collection and its further transfer at the electrode when needed is analyzed.

4.1 Single gate charge transfer

4.1.1 First structure

In this first structure the silicon bulk is n-doped.
A back side illuminated (BSI) photodiode at the center has been realized with an heavier n doping.
A shallow p layer is used to push electrons away from the oxide in order to avoid trapped charges.
At the sides of the structure floating diffusion (FD) electrodes are present for charge collection.
Two gate electrodes are used for the transfer of charge from the back side illuminated (BSI) photodiode to the floating diffusion electrodes (FD).
A p layer in the back is put for creating the junction to be depleted. Contact and deep p-well layers at the sides act as a barrier to prevent electron from going to the floating diffusion electrodes during the charge collection.

The doping levels are defined by companies' standards.

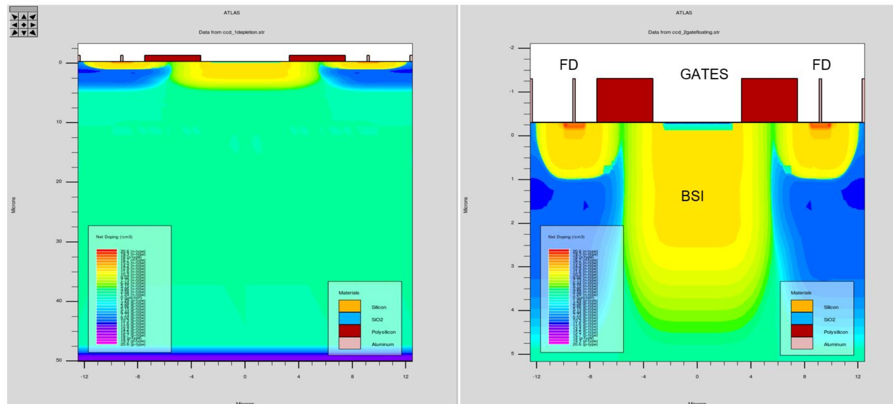

Figure 9: *Structure of the sensor*

Regarding the device simulation, as initial conditions, the back and the p-well electrodes at the sides are set always to a constant potential, equal to -5 V and -3 V respectively, in order to deplete the structure and have an effective barrier. As for the operation of the sensor, these are the steps which have been performed during the transient simulation:

- $t = 0$: Complete depletion of the structure, FD electrodes are at 0V, the gates are turned on to +5 V;
- $t = 10$ ns: FD electrodes are disconnected: the FD region is floating, the potential distribution in the structure stays due to its intrinsic capacitance;
- $t = 20$ ns: Blocking the transfer channels with the gates (0 V);
- $t = 30$ ns: Charge is generated in the center of the structure and collects in the BSI region;
- $t = 100$ ns: Transferring collected charge from the BSI region to the FD regions by turning on the gates (+5V);
- $t = 200$ ns: Blocking the channels by putting 0 V on the gates, in order to keep the transferred charges in the floating diffusion region and isolate it from the rest of the structure;

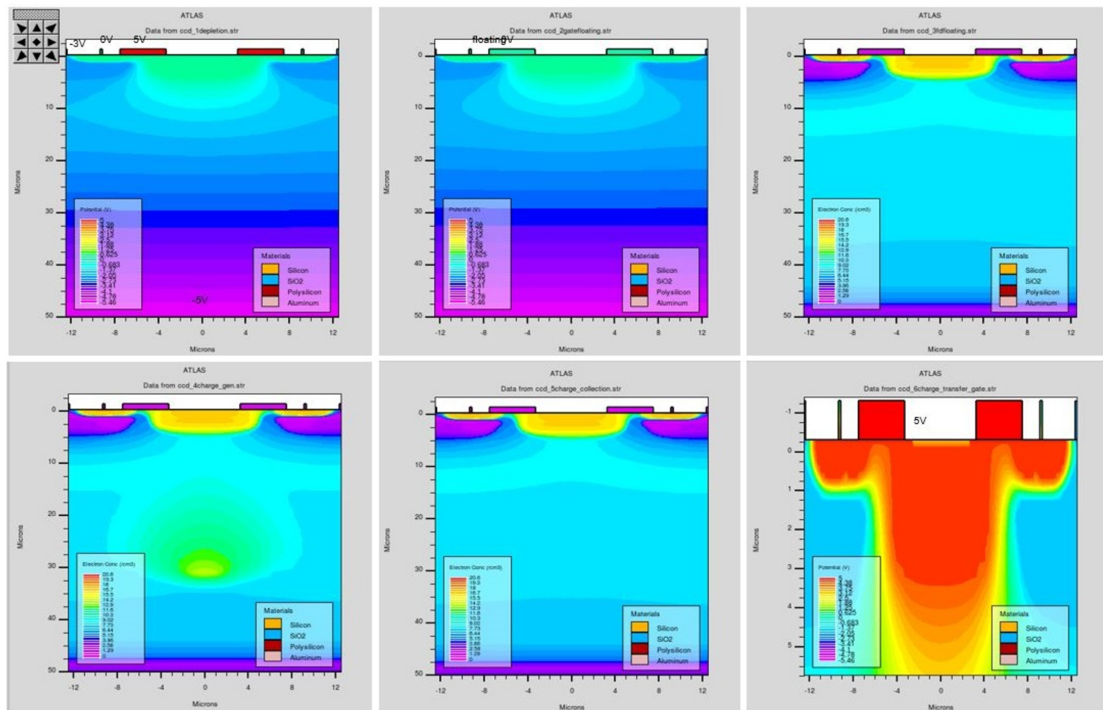

Figure 10: *Operation of the single gate sensor*

- $t = 300\ ns$: Closing the FD switch to collect the charge[2].

In figure 11 the potential profile along a cross section under the gate which goes horizontally along the width of the structure is shown, together with the charge collected at the FD electrodes, at the moment of the closing of the FD switch.

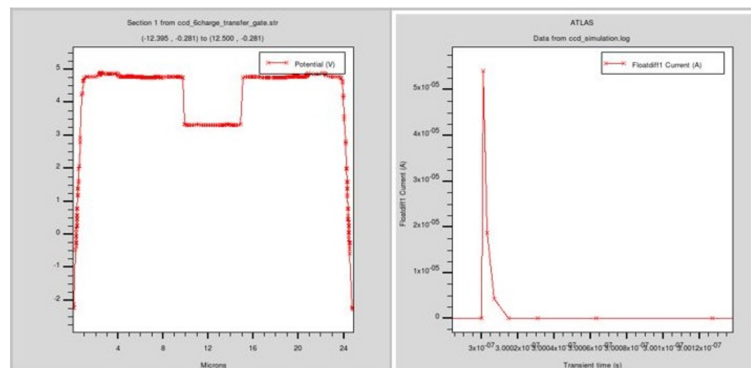

Figure 11: *Voltage profile during transfer and collected charge*

From the plotted cut-line it is evident that a real drift field which moves the charges from the BSI to the FD regions doesn't exist[3].

In fact, by turning the gates on, since the big n-region in the center of the structure is floating, it will follow the potential of the gates. The whole region is almost equipotential.

[2]This is done only for simulation purposes; in the real operation FD is always floating, the deposited charge is measured by observing the change in voltage of the FD region, known its capacitance, by means of a source follower.

[3]Notice that the central bump is due to the pinned layer and it's not representative of the potential of the BSI region.

4.1.2 Study of the potential profile during the charge transfer

The action on the gates was thought to modify the potential only of the zone immediately under them and not to change the potential of the whole n region.

In order to understand better this behavior, several simulations with different values of the gate voltage have been performed, following the same steps as the one sin section 4.1.1. In particular, the following values of the gate voltages for the charge transfer have been used: 2.5 V, 5 V, 7.5 V, 10 V, 15 V, 20 V, 30 V.

The plots represented in figure 12 show the potential profile on a cross section along the width of the structure immediately under the gate (where the blue line is) for different values of the gate voltage, during the charge transfer operation. The order in which they are reported follows the one written above (from left to right and from the top to the bottom).

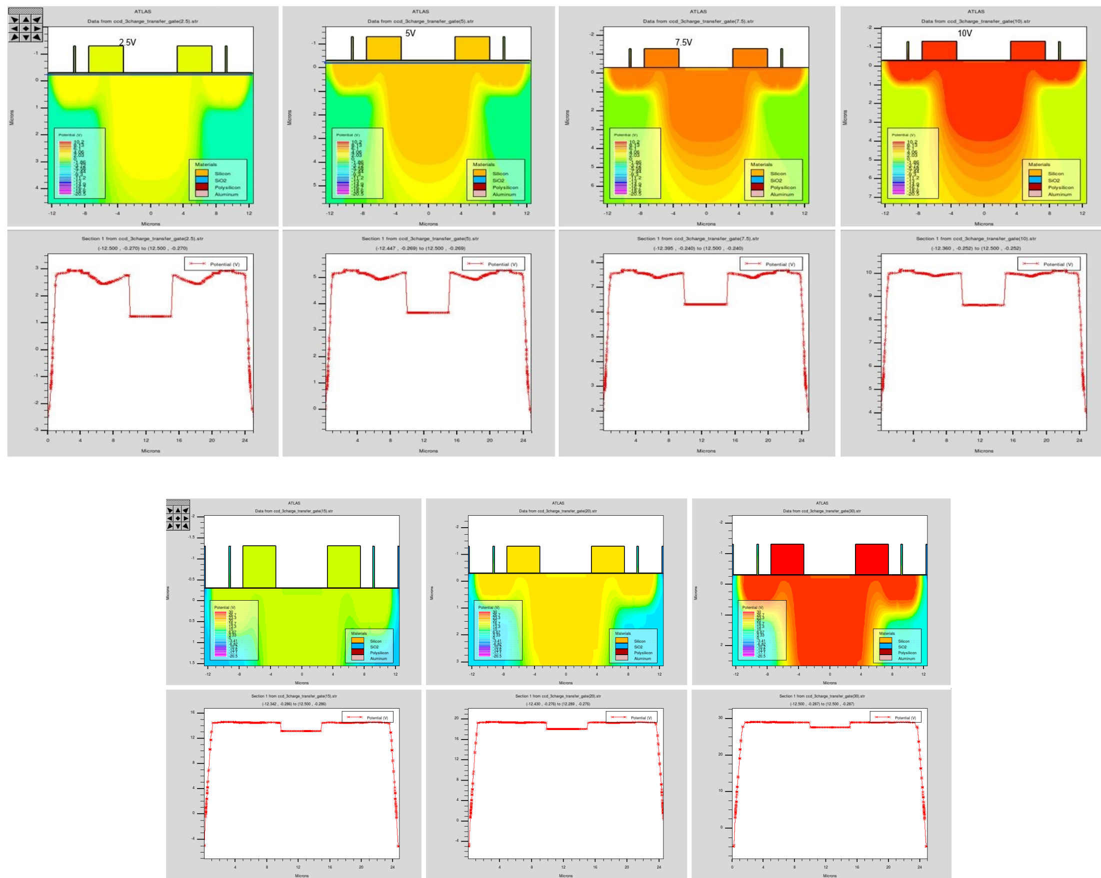

Figure 12: *Sweeping the gate voltage for charge transfer*

As you can notice, changing the gate voltage does not influence the potential difference between two points of the structure. It just shifts the potential of the whole floating n region, according to the voltage applied on the gates.

To overcome this problem, different solutions will be discussed in the following sections.

4.1.3 Resetting the FD electrode

One possibility to be analyzed is trying to reset the FD regions after blocking the channel with the transfer gates. In this way a potential difference between the BSI and the FD is created as initial condition, while in the previous case the whole structure reached the steady state condition and the whole n region became equipotential.

The whole operation of the sensor, then, has to happen before recombination happens, i.e. before the structure reaches again a steady state equipotential condition (time constant of the order of ms).

The constant voltages applied in this case are -20 V on the back and -10 V at the sides pwell electrodes. The timing of the operations now performed is the following:

- $t = 0$: Complete depletion of the structure, FD electrodes are at +3V, the gates are turned on to +3 V;
- $t = 10\ ns$: Blocking the transfer channels with the gates (-3 V), FD contacts are still reset at +3 V;
- $t = 20\ ns$: FD electrodes are disconnected: the FD region is floating;
- $t = 30\ ns$: Charge is generated in the center of the structure and collects in the BSI region;
- $t = 100\ ns$: Transferring collected charge from the BSI region to the FD regions by turning on the gates (+3V);
- $t = 200\ ns$: Blocking the channels by putting -3 V on the gates, in order to keep the transferred charges in the floating diffusion region and isolate it from the rest of the structure;
- $t = 300\ ns$: Closing the FD switch to collect the charge.

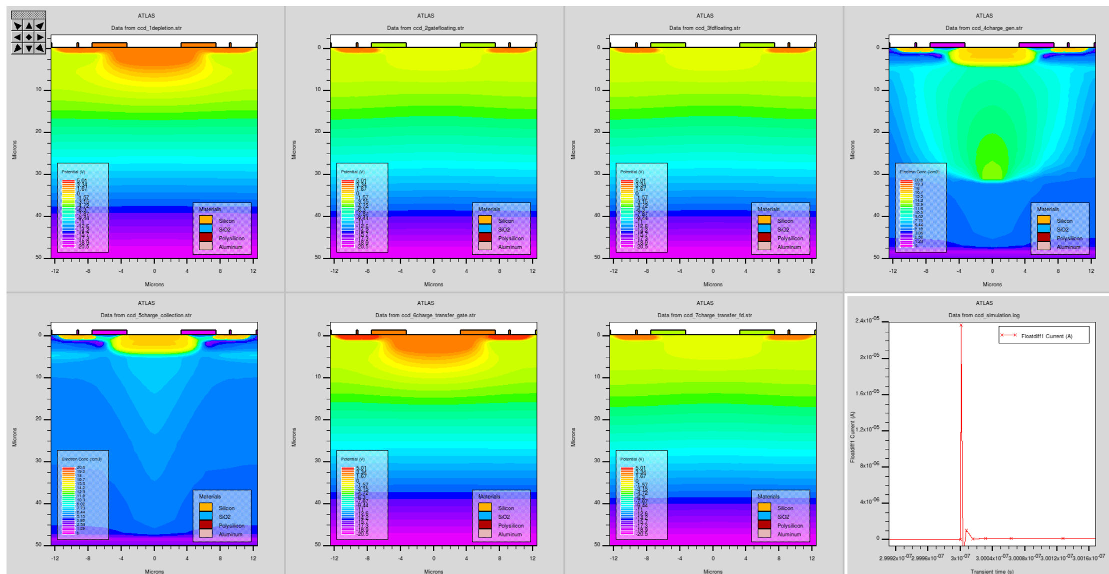

Figure 13: *Operation of the single sensor when FD is reset after blocking the channel*

In figure 13 the potential profile along a cross section under the gate which goes horizontally along the width of the structure is shown, while the sensor waits for charge to be generated.

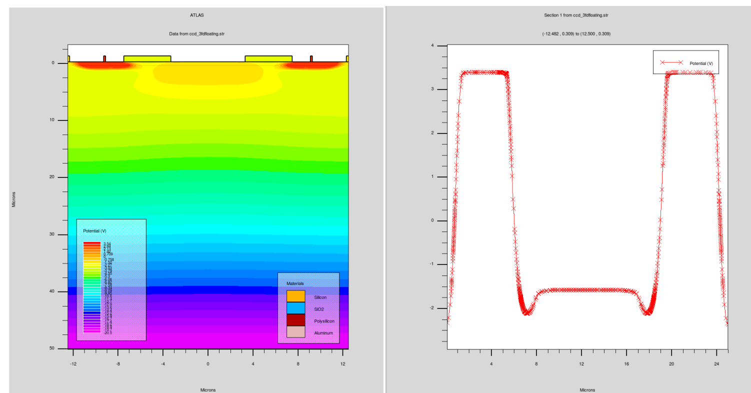

Figure 14: *Charge collection in the BSI*

The potential profile is not so good, since, during charge collection, electrons can go directly to FD instead of being collected in the BSI, due to the low potential bumps.

This can be easily fixed by isolating the FD and BSI regions better, by means of a p-doping.

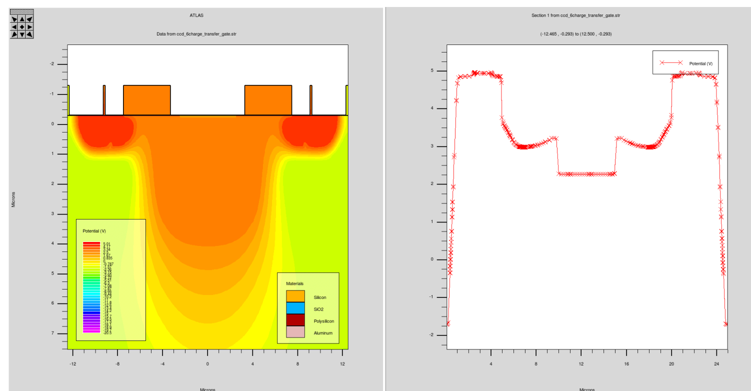

Figure 15: *Charge transfer from the BSI to the FD*

Conversely, the potential profile during the charge transfer really produces a drift field which moves electrons from the BSI to the FD. Notice that the potential of the whole floating n region shifts according to the transfer gate's voltage, but the general trend of the potential differences between points inside it is preserved.

Actually the operation described above is the same that is implemented in CMOS and CCD sensors when electrons need to be transferred to the FD.

4.2 Charge transfer with BSI gate

Here, with reference to the results reported in sections 4.1.1 and 4.1.2, the idea is to change the voltage distribution along the horizontal cross section of the structure with respect to the previous case by means of an additional gate placed over the BSI region.

Before, the structure became equipotential following the transfer gate voltage; here I try to move the potential of particular points of the structure with respect to others by playing with more than one gate.

Clearly, the floating pinned layer placed over the BSI region has to be removed.

No voltage resetting is applied.

4.2.1 TCAD simulation

In figure 16, the new proposed structure is represented.

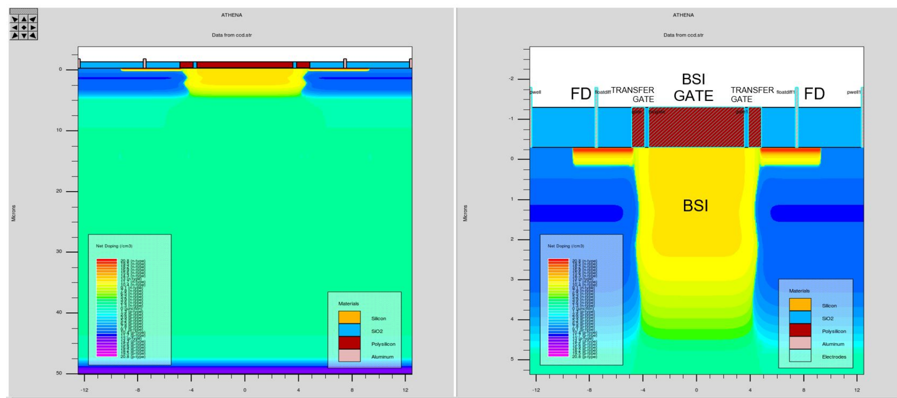

Figure 16: *Structure of the sensor with the additional BSI gate*

The constant voltages applied in this case are -20 V on the back and -10 V at the sides pwell electrodes. The timing of the operations now performed is the following:

- $t = 0$: Complete depletion of the structure, FD electrodes are at 0 V, the gates are turned on to +5 V;
- $t = 10$ ns: FD electrodes are disconnected: the FD region is floating;
- $t = 20$ ns: Blocking the transfer channels with the side transfer gates (-5 V); the BSI gate is still at +5 V;
- $t = 30$ ns: Charge is generated in the center of the structure and collects in the BSI region;
- $t = 100$ ns: Transferring collected charge from the BSI region to the FD regions by turning on the gates: first 0 V on the BSI gate, then +5 V at the transfer gates, finally -5 V on the BSI gate;
- $t = 200$ ns: Blocking the channels by putting -5 V also on the BSI gate;
- $t = 300$ ns: Closing the FD switch to collect the charge.

In figure 17 the TCAD simulation of the depletion of the sensor is shown. After that the BSI gate is kept on in order to help attracting the generated electrons in the BSI region.

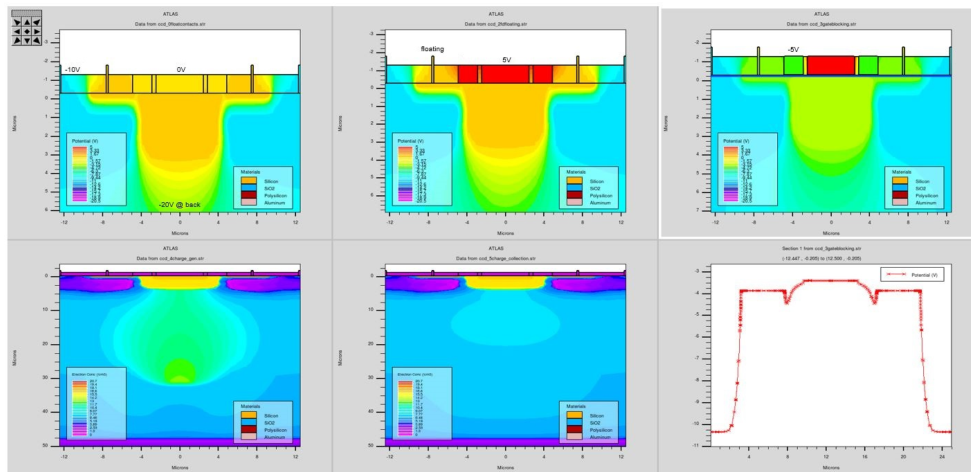

Figure 17: *Preconditioning of the structure, charge generation and collection in the BSI*

In figure 18, the operation performed for the charge transfer are represented. At first the BSI gate's potential is lowered to 0V, then the transfer gates' potential is increased up to +5V, finally the BSI gate's voltage is put to -5 V in order to push electrons toward the FD regions.

In this case there is clearly a more evident drift field which moves charges from the BSI to the FD regions. However the potential differences which are responsible of that are of the order of hundreds of millivolts.

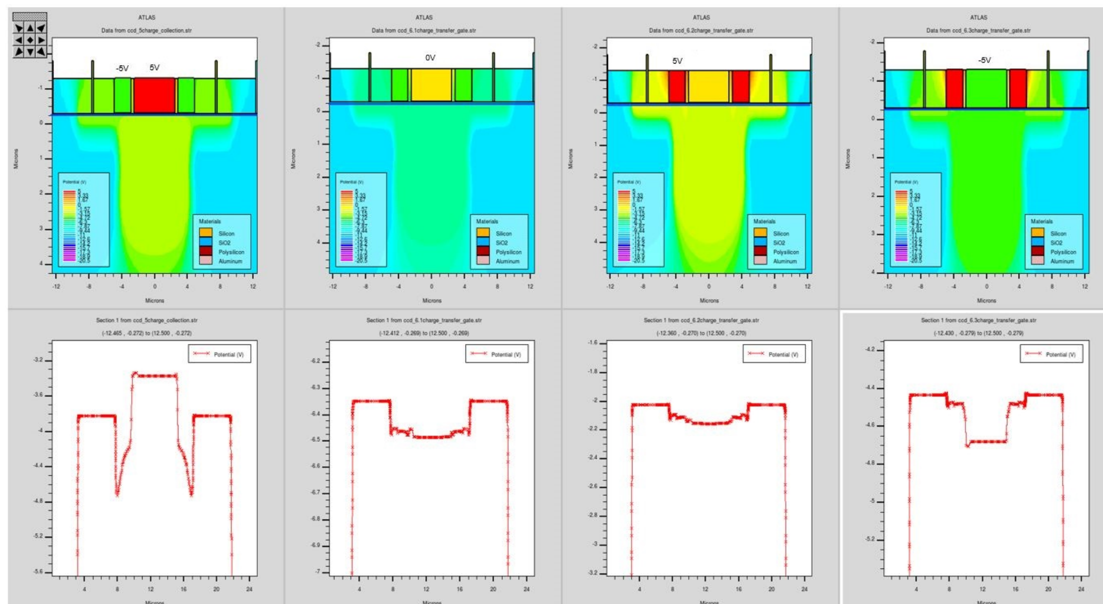

Figure 18: *Charge transfer from the BSI to the FD*

Finally, in figure 19, all the gates are in the blocking state and the FD switch is closed to collect the transferred charge.

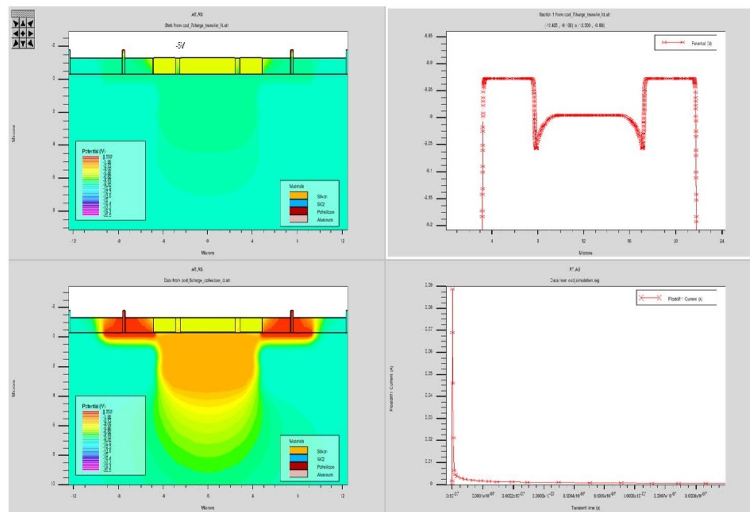

Figure 19: *Charge collection at the FD electrodes*

In figure 20 the voltages of every electrodes as a function of time are shown.

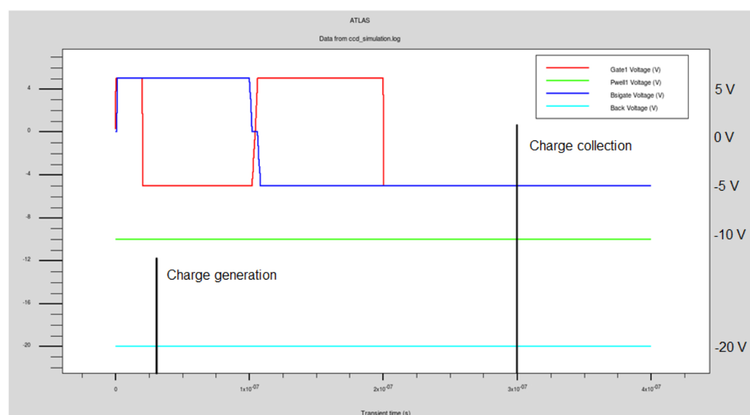

Figure 20: *Timing of the operations performed*

4.2.2 Charge collection verification

Between the moment in which FD electrodes are made floating and the moment in which they are again connected to the structure for charge collection there is a different state of the gate electrodes which are capacitively coupled with the whole structure. For this reason the current measured at the FD electrode is affected also by the transient of the structure which wants to find another equilibrium condition.

Given this consideration, the verification of the charge collection is done by comparing two simulations: with and without charge generation.

The generated charge is computed as the charge carried by the holes that drift immediately to the back of the structure as soon as electron hole-pairs are generated by x-rays.

The collected charge is conversely computed as the difference between the charge flowing through the floating diffusion electrode with and without the charge generation.

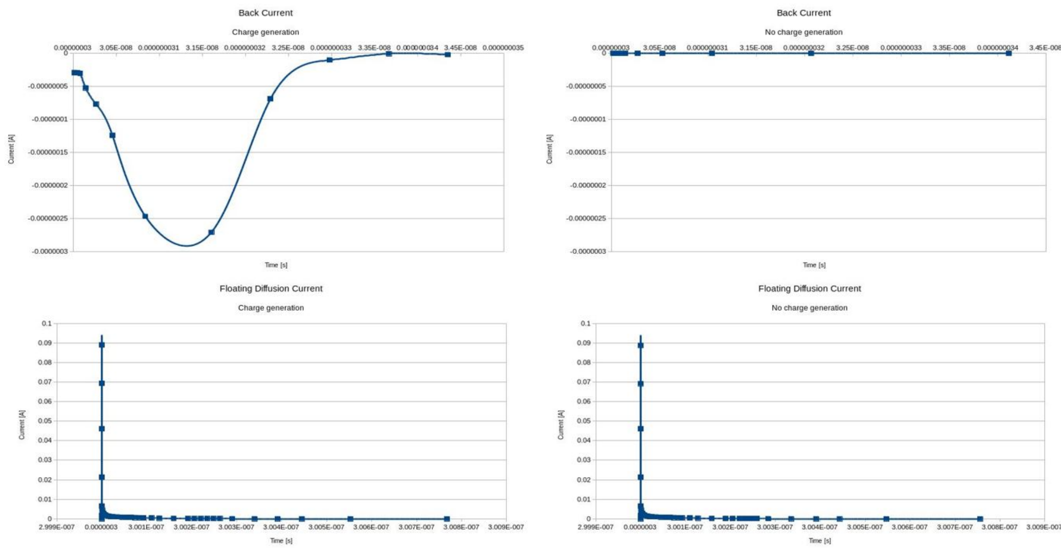

Figure 21: *Charge collection verification process*

From this device an error of 10% is reached, which is an acceptable result, given the accuracy of the simulation.

4.3 Charge transfer with a J-FET structure

In this section I am analyzing a J-FET-like stage for the charge transfer, in order to make it happen more deeply in the structure and avoid electrons trapped on the oxide surface.

4.3.1 Proposed structure

With the standard doping levels at my disposal, the only possible structure to perform the transfer of charge with the J-FET-like stage is shown in figure 22. An important requirement for its correct operation is that the channel must be uniformly doped.

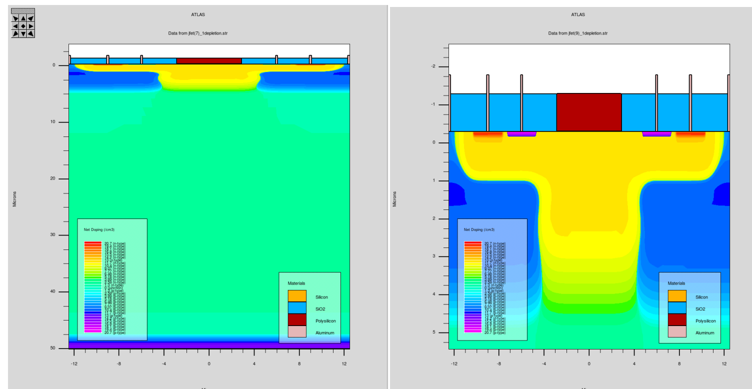

Figure 22: *Structure of the J-FET-like stage sensor*

The idea for the operation of this sensor is to close the channel by applying a negative voltage on the new J-FET electrode (in contact with the p implant) when the charges have to be collected in the BSI region.
After that the charge transfer is performed by releasing the J-FET gate's voltage in order to open the channel and let electrons flow from the BSI region to the FD regions.

4.3.2 Study of the potential needed to close the channel

An analysis of the potential which is necessary to have the channel closed is performed in figure 23. The FD electrodes are always floating after the structure has been depleted.

The used voltages for the J-FET electrodes are: -10 V, -20 V, -30 V, -40 V, -50 V, -60 V, -70 V, -80 V, -90 V. They are represented from left to right and from the top to the bottom in the same order written above.

In order to allow this range of voltage for the pimp electrodes, the voltage at the back is always fixed at -100 V, while the voltage at the pwell side electrodes is always fixed at -90 V.

The plots represented are related to a device simulation analogous to the previous ones. In particular the situation in which the channel is blocked after the structure has been depleted and the FD has made floating is represented.
After that the sensor waits for charge to be collected in BSI region to further transfer it to FD by acting on the J-FET channel.

From the plots it is evident that an acceptable potential profile is not present till a voltage equal to -30 V is applied to the electrode, which is far too much with respect to the voltage ranges which are used in these applications.

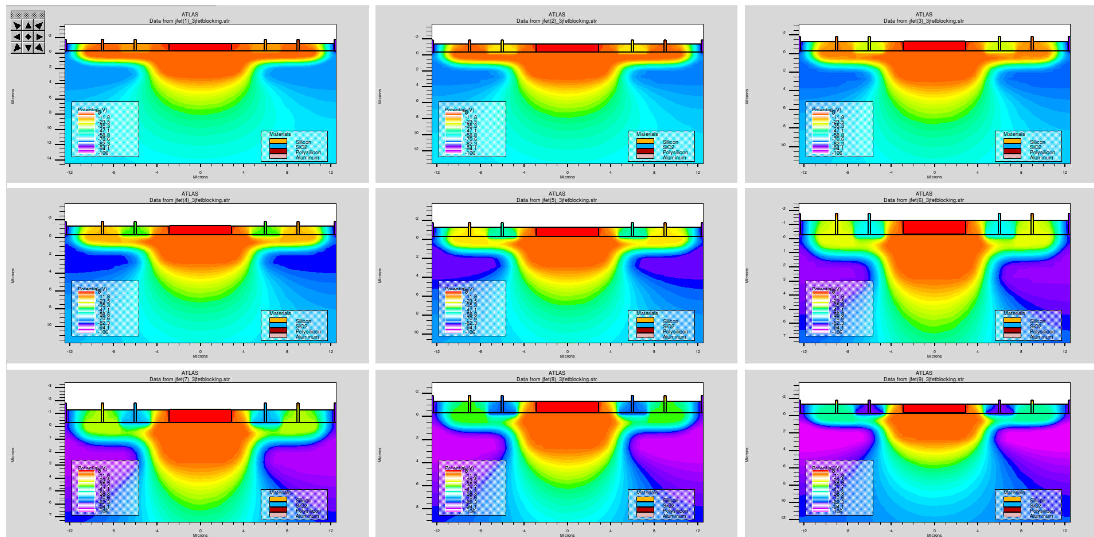

Figure 23: *Study of the potential needed to close the channel*

This problem can be fixed essentially by lowering the width of the channel. This is possible in two ways, either by reducing the depth of the n-well layer or by increasing the depth of the p-implant.
For both these solutions a new doping level has to be developed ad-hoc.

For this reason this topic is left pending, paving the way for further developments.

4.4 Pinned diode experiment

In this part another version for the charge transfer from the BSI to the FD is developed[4].
It relies on a pinned photo-diode, i.e. the back side illuminated photo-diode is constituted also by a pinned layer on the top kept at a fixed potential.

With respect to the sensor developed in section 4.1.1, the main difference is that the pinned layer now is enriched with an ohmic contact which fixes its potential at a constant value.

This creates a diode whose anode and cathode are the pinned layer and the BSI n region respectively. The diode is always operated in reverse biased conditions, however the BSI region in any case cannot reach a potential which is lower than the one of the pinned layer minus the built-in potential of the diode ($\simeq 0.7\ V$), that is the moment in which the diode starts conducting.

Thanks to this idea, I have fixed the lower limit for the potential of the BSI region.

In figure 24, the proposed structure is represented.

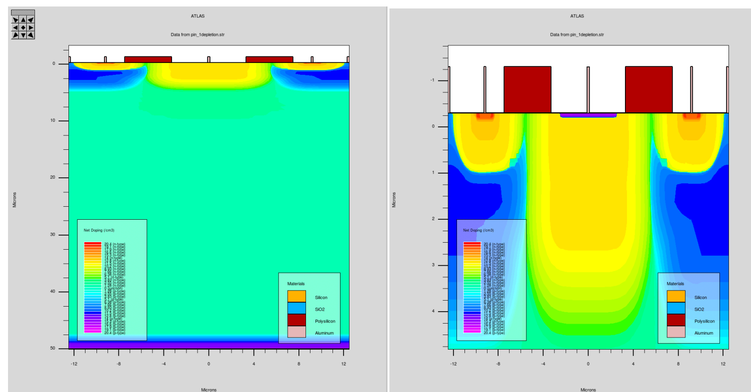

Figure 24: *Structure of the sensor with pinned diode*

The constant voltages applied in this case are -20 V on the back, -10 V at the sides pwell electrodes and 0 V at the electrode connected to the pinned layer. No FD resetting is applied. The timing of the operations now performed is the following:

- $t = 0$: Complete depletion of the structure, FD electrodes are at +3 V, the gates are turned on to +3 V;
- $t = 10\ ns$: FD electrodes are disconnected: the FD region is floating;
- $t = 20\ ns$: Blocking the transfer channels with the side transfer gates (-3 V);
- $t = 30\ ns$: Charge is generated in the center of the structure and collects in the BSI region;
- $t = 100\ ns$: Transferring collected charge from the BSI region to the FD regions by turning on the gates (+3 V);
- $t = 200\ ns$: Blocking the channels by putting -3 V also on the BSI gate;
- $t = 300\ ns$: Closing the FD switch to collect the charge.

In figure 25 the TCAD simulation of the operation of this new version of the sensor is shown.

[4] I have developed the simulation about this after the problems coming from the simulation of the first final version of the FLORA PIXEL exposed in section 6. I put it in this part for coherence with the rest of the topics.

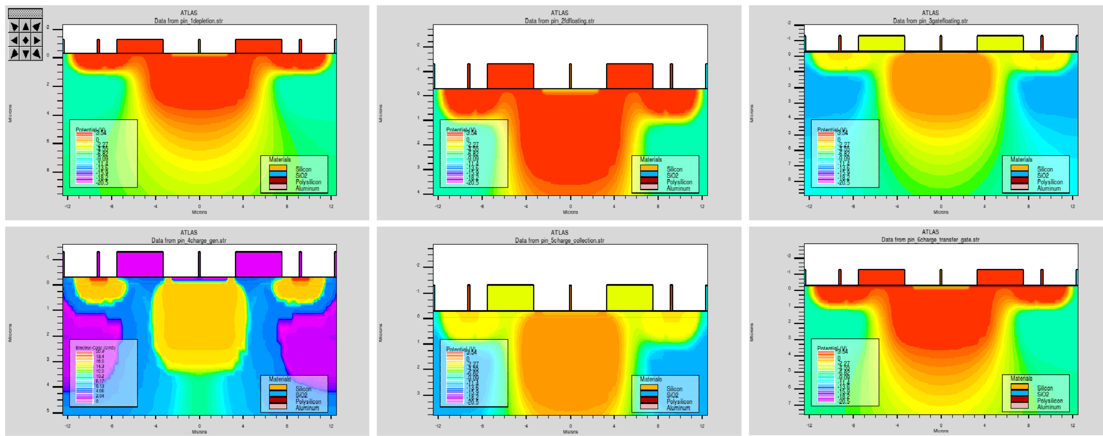

Figure 25: *Device simulation of the operation of the pinned-diode-like sensor*

The advantage of the pinned photo-diode with respect to the situation described in section 4.1.1 is that, the potential of the BSI limit cannot go below a certain value, fixed by the voltage of the pinned layer. Hence, during blocking, it's potential stays up and this creates a very nice potential profile for charge collection.

As for the charge transfer, there are no differences with respect to section 4.1.1, because even if the potential of the BSI region cannot go down, it can still go up like before. For this region, even in this case, during transfer, there is not really a drift field which moves electrons (this can be fixed by resetting the FD electrode every time).

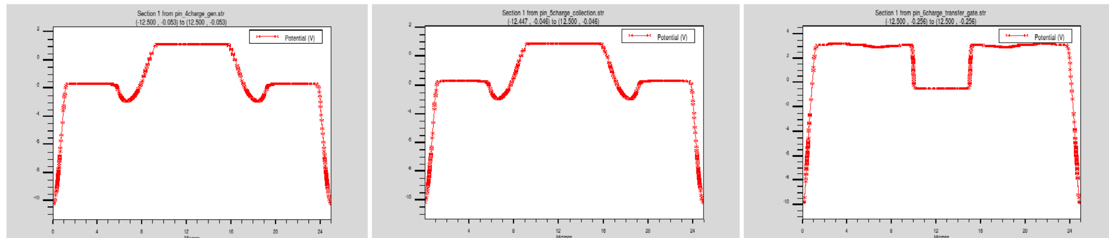

Figure 26: *Horizontal potential profile during charge generation, collection and transfer*

In figure 26 the potential profile along an horizontal cutline under the gates is shown. Notice that, as in every case, the potential of the BSI region lower when charges collect there.

After all these analyses, the simulation of the final sensor is developed and described in detail.
The knowledge coming from the understanding of the working principle of the devices shown till now allowed me to put all bricks together and develop a final version of the FLORA PIXEL sensor.

Part III
FLORA PIXEL

In this part a final working version of the FLORA PIXEL will be proposed.
Thanks to the results and the studies of the previous devices, it has been possible to develop a final version of the sensor.

5 Introduction of the overflow electrode

The structure of the complete sensor is built in reference to the scheme initially proposed.
In fact, in this case, given the necessity to provide a double path for charges, only one FD electrode is present at the center, while to BSI regions are placed at its sides, from where the collected electrons go either to the FD or to the overflow electrode.

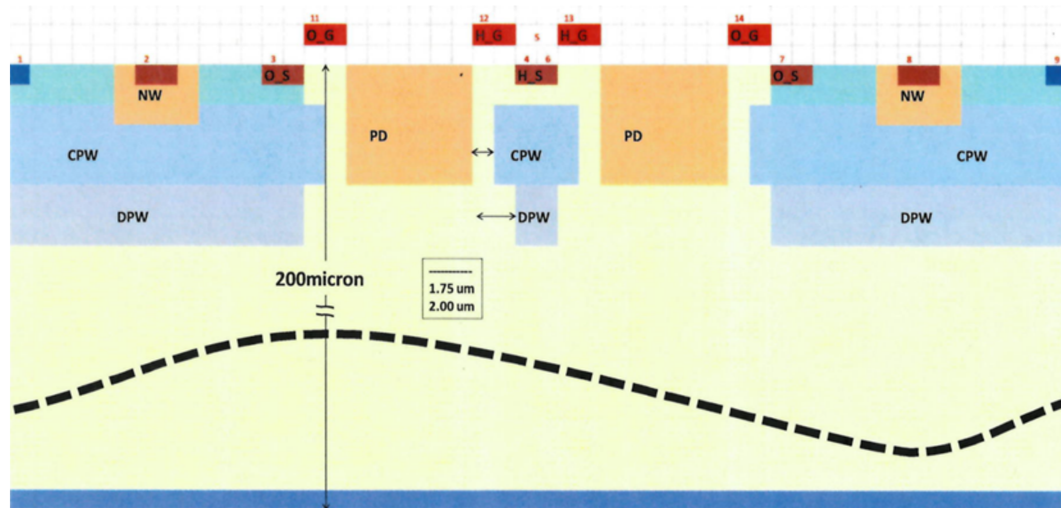

Figure 27: *FLORA pixel proposal*

The sensor is hence provided with to electrodes for charge measurements:

- **Floating Diffusion electrode**: Charges collect in the BSI and are further transferred in the central FD region, which has a smaller capacitance, given its reduced dimensions. Charge will be measured by a source follower which will observe the change in voltage of the floating diffusion region before and after charges gather there. This is the high sensitivity electrode, used to measure small amounts of charges.

- **Overflow electrodes**: In presence of a large X-ray signal, an high amount of charge is generated in the silicon. The BSI region can host only the charge amount which can be measured by the floating diffusion electrode (defined by the possible range of potential variations of the FD region). The charge exceeding this threshold will flow continuously to the sides, through the overflow electrode. There, charge will be measured thanks to an integrator (operational amplifier with a feedback capacitance), which will provide virtual ground and hence will keep the overflow electrode at a constant potential (contrary to the FD electrode, I remind that it's floating).

Let's now analyze different proposed solutions for the realization of the structure.

6 Charge transfer with a BSI gate

6.1 Structure

After the positive results of the device simulated in section 4.2, the first attempt is try to add the overflow electrode to the structure with the BSI gate.

In figure 28, the proposed structure is represented.

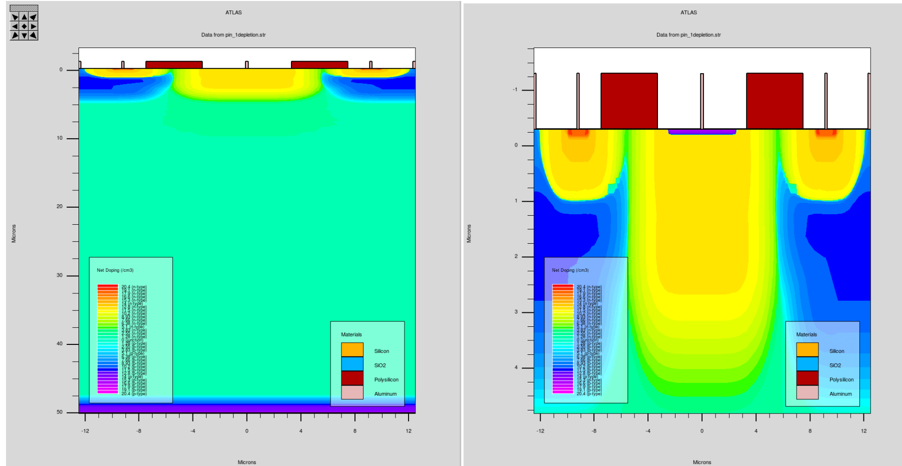

Figure 28: *First proposal of the FLORA PIXEL sensor*

6.2 Device TCAD simulation

Here, there is the overflow electrode which is kept at a constant potential.

The constant voltages applied in this case are -20 V on the back and -10 V at the sides pwell electrodes. The operations now performed is the following:

- $t = 0$: Complete depletion of the structure, FD electrodes are at 0 V, the gates are turned on to +3 V;
- $t = 10$ *ns*: FD electrodes are disconnected: the FD region is floating;
- $t = 20$ *ns*: Blocking the transfer channels to FD with transfer gates (-3 V); the overflow gates are instead put to -1 V; the BSI gate is still at +3 V;
- $t = 30$ *ns*: Charge is generated in the center of the structure and collects in the BSI region;
- $t = 100$ *ns*: Transferring collected charge from the BSI region to the FD regions by turning on the gates: first +3 V at the transfer FD gates, then -3 V on the overflow gate to block the overflow channel, finally +2 V in the BSI gate to push electrons from there to the FD, creating a kind of voltage staircase;
- $t = 200$ *ns*: Blocking the channels by putting -3 V also on the BSI gate;
- $t = 300$ *ns*: Closing the FD switch to collect the charge.

In figure 29 the TCAD simulation of the depletion, charge generation and collection is shown.

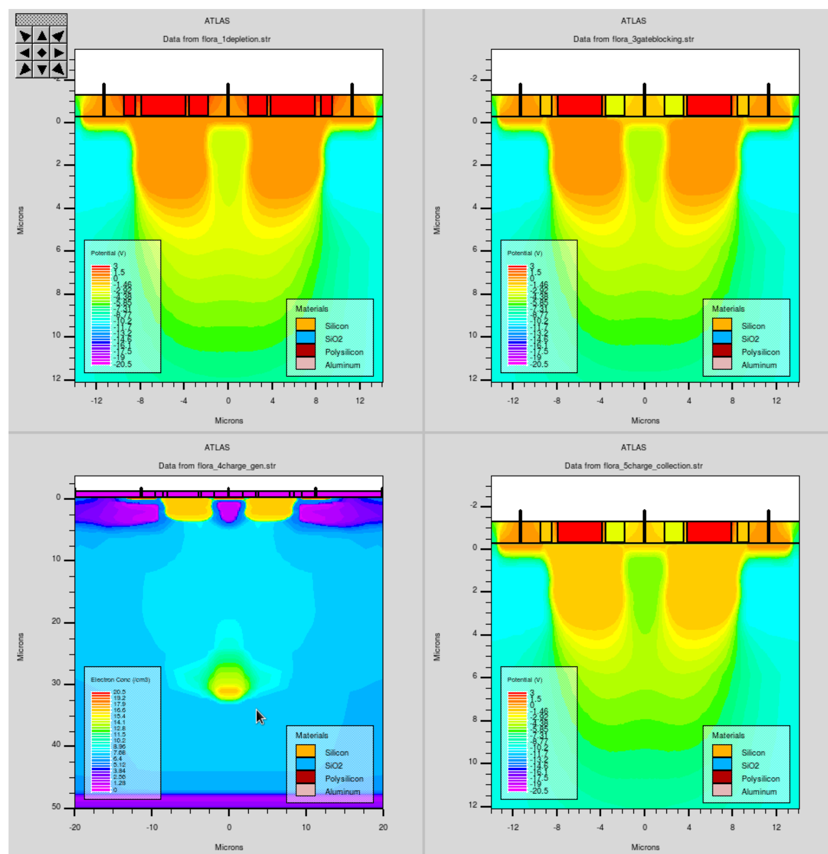

Figure 29: *FLORA with BSI gate: Depletion, charge generation, collection and flow to the overflow*

A very high amount of charge has been generated to test the overflow electrode. In fact, charge which collects in the BSI region lowers its potential, until it gets at the same level as the potential of the bump provided by the overflow gate. At this point, the exceeding charges will start flowing through the overflow electrode. In figure 30 the overflow and the back current are represented together with the potential profile before and after charge collection in the BSI. This version, hence, realizes correctly the continuous charge flow through the overflow electrodes.

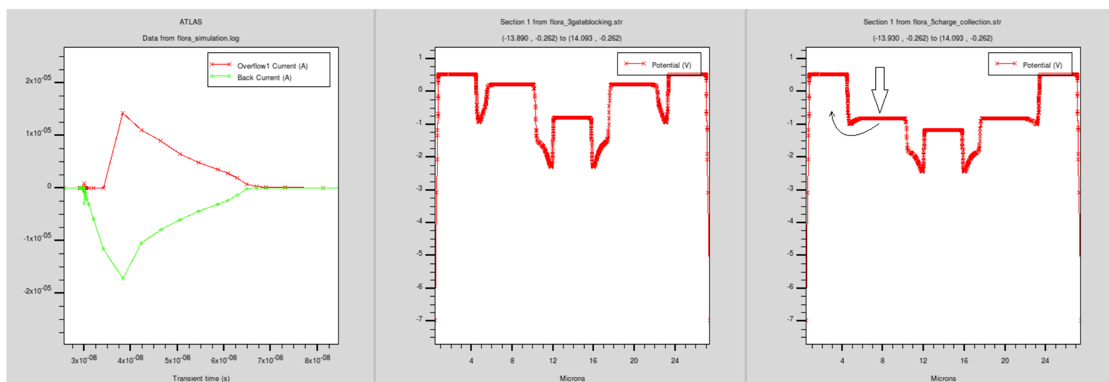

Figure 30: *FLORA with BSI gate: continuous charge flow in the overflow electrode*

As for the transfer of the remaining charge (figure 31) which is still in the BSI, from this simulation it's clear that the charge collected in the BSI is too much, so that when it's transferred

to the FD, it lowers significantly its potential and then it spreads around the big n area formed by the BSI and the FD regions, which becomes almost equipotential. Finally the voltage of the overflow gate must be tuned in order to allow the right amount of charges in the BSI, which then can be hosted even by the FD electrode.

Moreover, during these operations, the BSI gate is heavily influenced by the blocking action of the overflow gates: its potential drops down and charges will flow automatically to the overflow electrodes instead of going to the FD region.
I did other trials reducing the dimensions of the overflow gates and increasing the ones of the FD gates, but without significant differences.

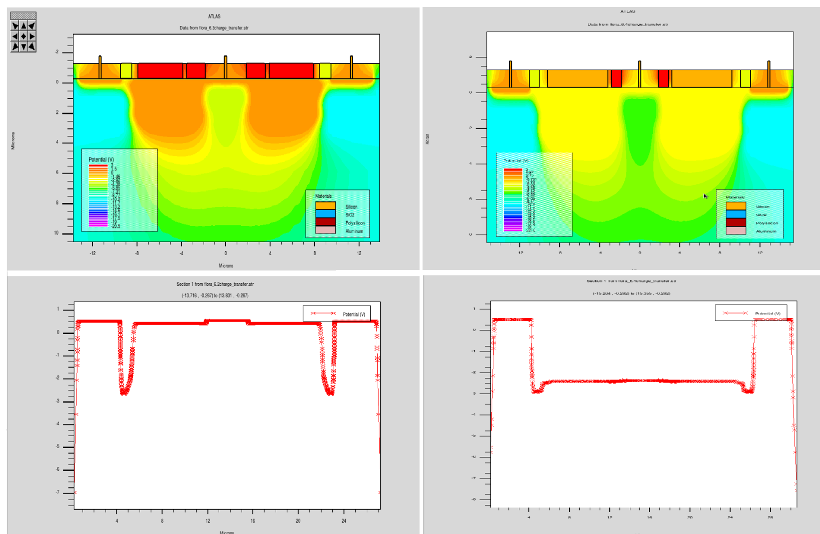

Figure 31: *FLORA with BSI gate: charge transfer from the BSI to the FD*

Even a simulation without charge generation has been tried (figure 32), but no significant changes in the distribution of the potential have been found, meaning that another solution for the charge transfer must be developed.

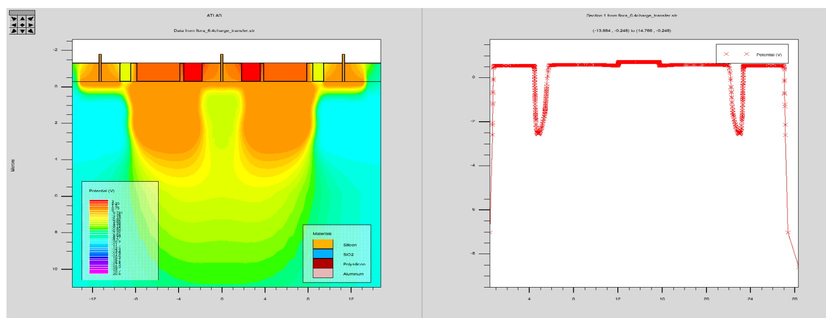

Figure 32: *FLORA with BSI gate: charge transfer from the BSI to the FD without charge generation*

After that, the BSI to FD channel is blocked by the transfer gates (figure 33) and charge is collected at the FD electrode. Clearly, for the reasons described before, only a fraction of the whole charge deposited in the BSI is collected.

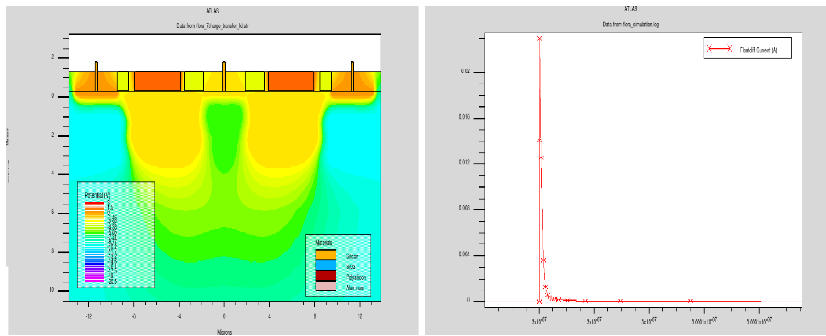

Figure 33: *FLORA with BSI gate: charge collection at the FD electrode*

After these considerations, the pinned diode experiment (which has been exposed in the previous part, section 4.4) has been developed and analyzed in order to correct the problems that arise from the operation of this device, in particular the sink of potential of the BSI region.

It must be clear that this device can still be improved and tuned correctly. A further analysis of this possibility is left to the reader.

7 FLORA PIXEL: final version with pinned photodiode

The following proposal for the FLORA PIXEL has been realized thanks to the combination of the results obtained till now. This will lead to a final proposal for the sensor, which concludes my work of the past two months.
Clearly the sensor can still be improved and optimized.
I will provide suggestions and hints in order to allow others to develop my work further.

7.1 Structure and device simulation

In this version, the pinned layer above the BSI region is kept at a constant potential. Moreover in this case, the FD region is reset when the transfer channels are blocked; then it's made floating.

In figure 34, the proposed structure is represented.

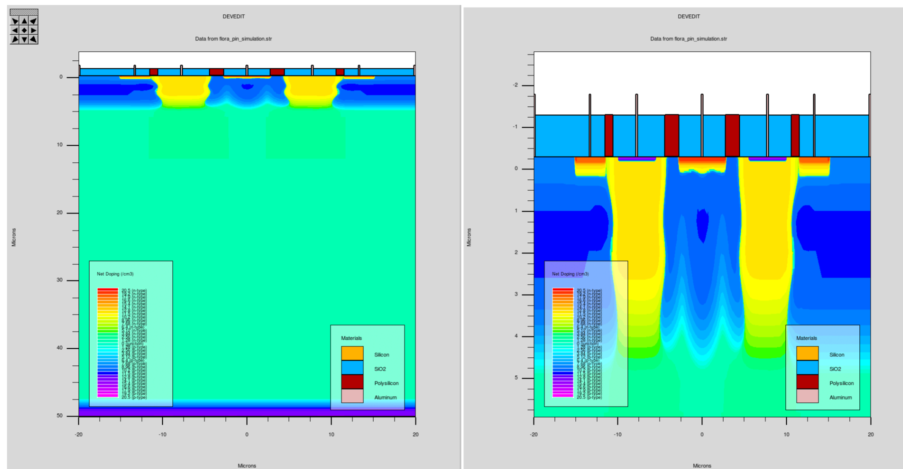

Figure 34: *Pinned photodiode version of the FLORA PIXEL sensor*

7.2 Device simulation: small signals

The constant voltages applied in this case are -20 V on the back, -10 V at the sides pwell electrodes and -2 V at the pinned layers. The operations now performed is the following:

- $t = 0$: Complete depletion of the structure, FD electrodes are at +3 V, the gates are turned on to +3 V;
- $t = 10$ ns: Blocking the transfer channels to FD with transfer gates (-3 V); the overflow gates are instead put to 0.5 V; the BSI gate is still at +3 V;
- $t = 20$ ns: FD electrodes, just reset, are disconnected: the FD region is floating;
- $t = 30$ ns: Charge is generated in the center of the structure and collects in the BSI region;
- $t = 100$ ns: Transferring collected charge from the BSI region to the FD regions by turning on the gates (+3 V);
- $t = 200$ ns: Blocking the channels by putting -3 V also on the BSI gate;
- $t = 300$ ns: Closing the FD switch to collect the charge.

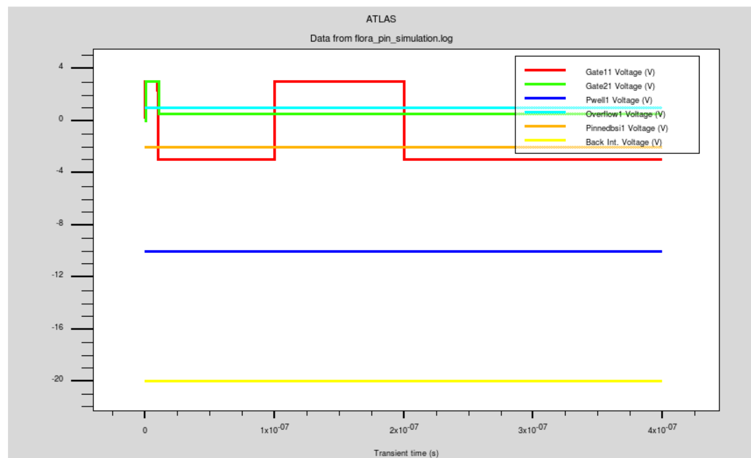

Figure 35: *Time diagram of the performed operations*

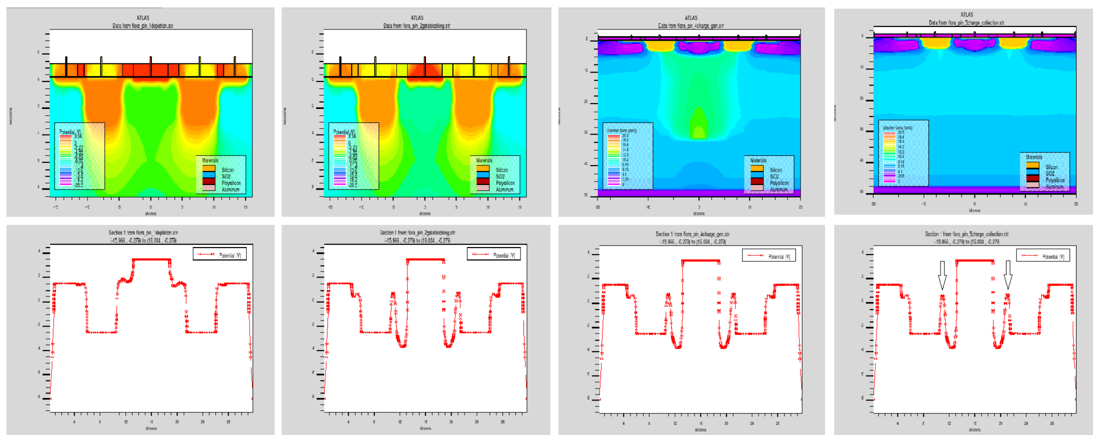

Figure 36: *FLORA with pinned diode: Depletion, charge generation, collection*

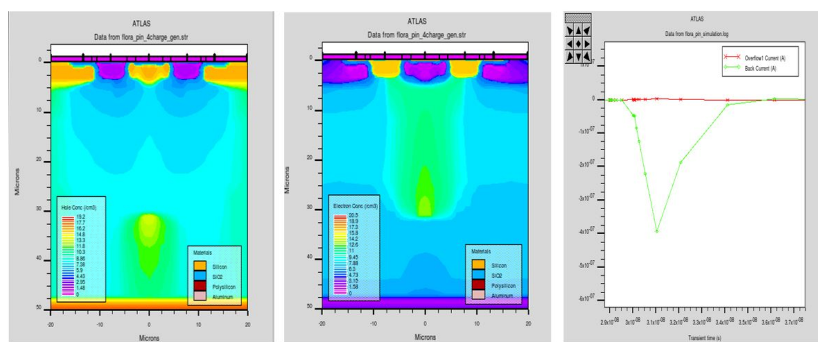

Figure 37: *FLORA with pinned diode: Depletion, charge generation, collection*

The structure is completely depleted while all gates are turn on. Then the transfer channels are blocked and the FD electrodes are reset before floating. The generated charge collects in the BSI region and lower its potential.
In this simulation it is not sufficient to activate the flowing through the overflow electrode (figure 37).

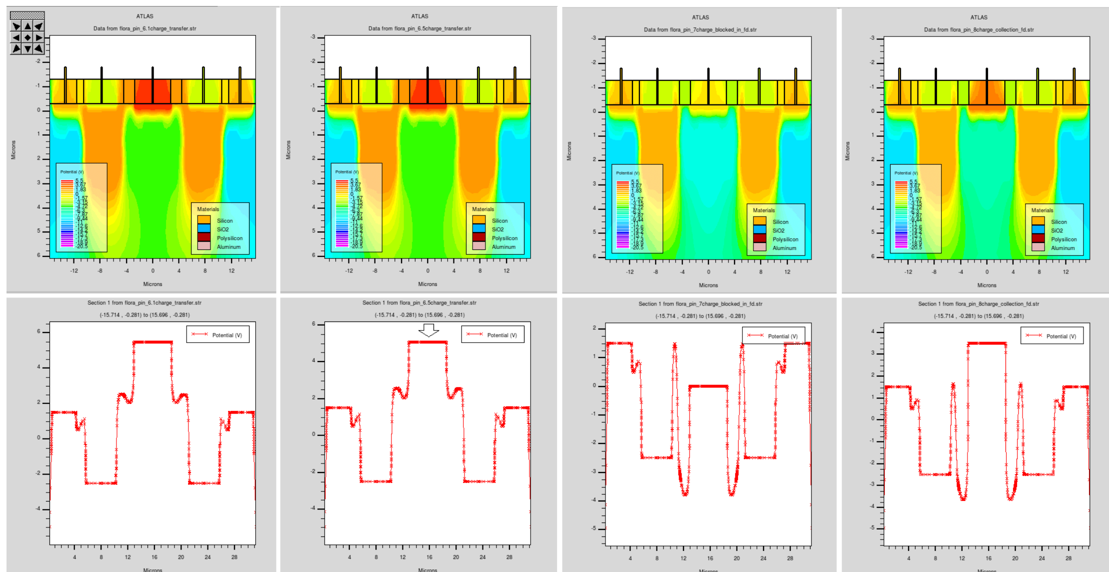

Figure 38: *FLORA with pinned diode: charge transfer from the BSI to the FD, blocking and collection at the FD electrode*

From the BSI charges are transferred to the floating diffusion region by means of the transfer gates. Thanks to the FD resetting, a potential difference between BSI and FD exists. Once charges are collected in the FD region, its potential lowers.
Then the transfer channels are blocked to isolate the FD region, before closing the switch.

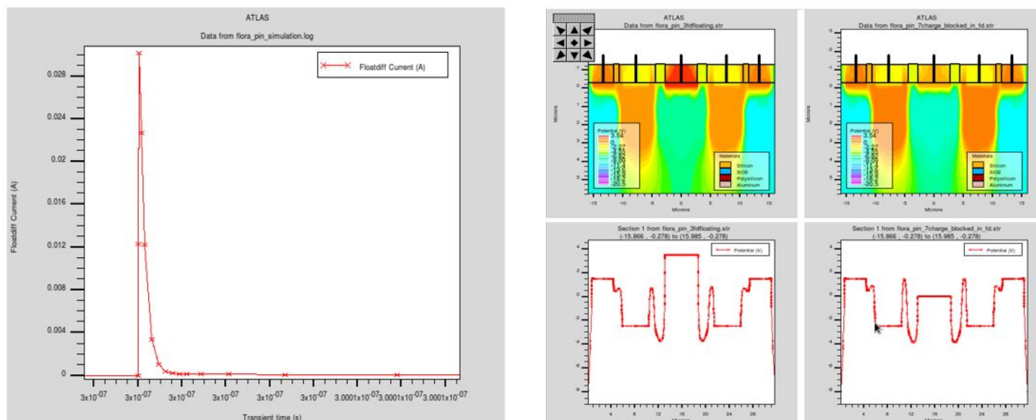

Figure 39: *FLORA with pinned diode: charge measurement modes*

After the floating diffusion switch is closed, charge is collected at the electrode. This is done only for simulation purposes: in the real operation of the sensor the floating diffusion region is always floating. Charge is measured by looking at the voltage difference of the FD region before and after charge collects there, known the (small) capacitance of the region.

The charge which provokes the maximum variation in voltage of the FD region constitutes a limit for the capacity of the BSI.
The overflow electrode's voltage must be set in order to allow in the BSI an amount of charges which does not saturate the FD region.

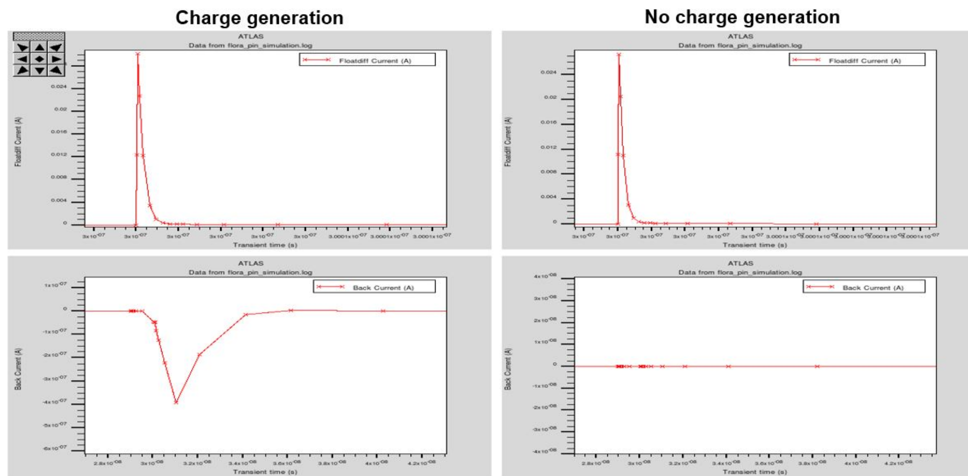

Figure 40: *FLORA with pinned diode: charge measurement verification*

Even in this case two simulations are performed in order to compute the collected charges: with and without charge generation. A comparison of the difference between the charge collected at the back in the two situations and the difference between the charge collected at the front is performed. In this case an error of about 30% is obtained between charges collected and FD and charges collected at the beginning in the BSI.

7.3 Device simulation: large signals, overflow electrode

In this case simulations analogous to the previous one are performed.
The difference is that now higher amounts of charges are generated in order to activate the continuous charge flowing through the overflow electrode.

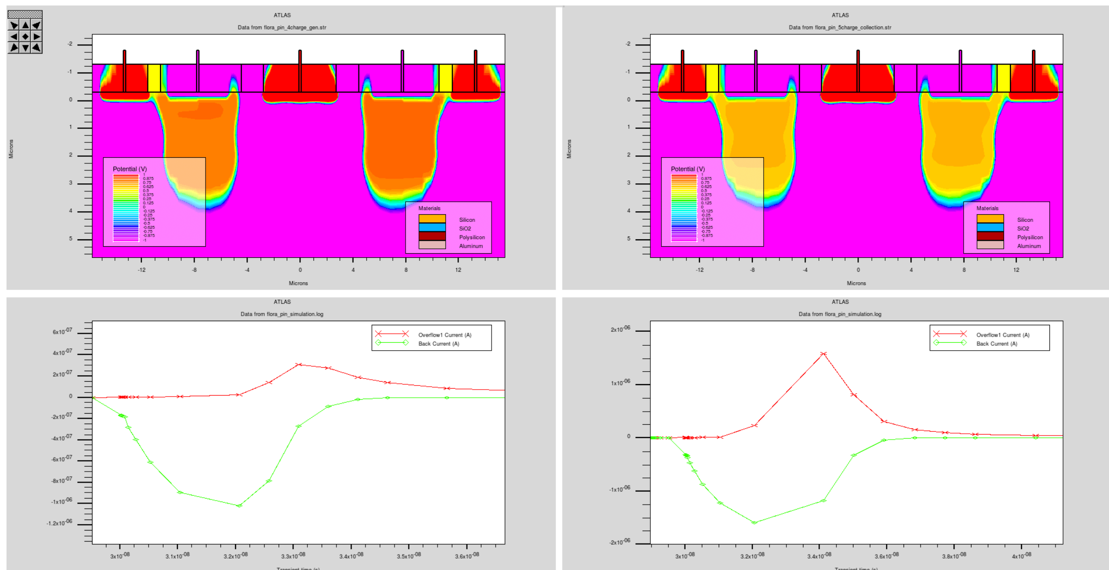

Figure 41: *FLORA with pinned diode: Continuous charge flowing*

Charges gather in the BSI region and lower its potential.

If many charges are generated, the BSI potential lowers till it reaches the value fixed by the overflow gates. In this case charges will overcome the bump and flow continuously through the

overflow electrodes, just after they are generated. Two different amounts of generated charges with the same threshold are represented in the bottom of figure 41.

7.3.1 BSI charge capacity

It's possible to modulate the charge capacity of the BSI acting on the overflow gate voltage. Its limit is fixed by the amount of charges that, in the further transfer, won't saturate the FD region.

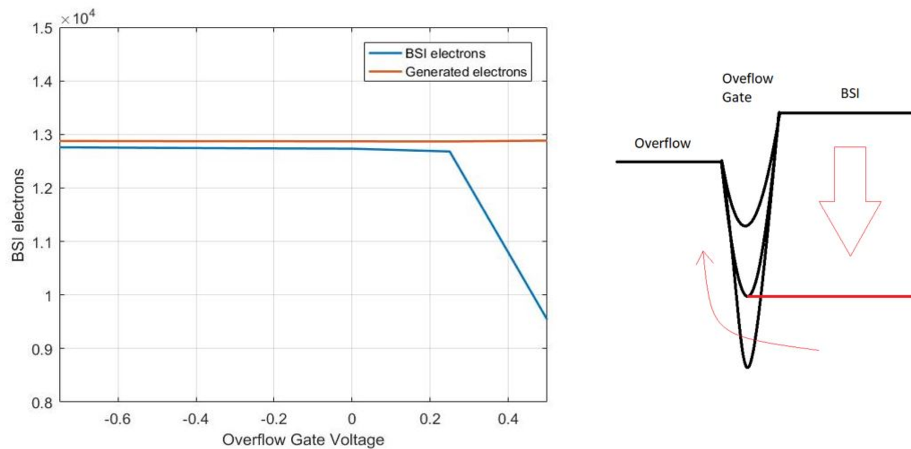

Figure 42: *FLORA with pinned diode: looking for the overflow activation threshold*

In any case, according to the desired number of electrons in the BSI region, the overflow gate voltage must be regulated.

The important role of the pinned diode is the one of not allowing the BSI potential to go down during blocking. Actually it fixes the lowest limit for the BSI potential.

In figure 42 the results of simulations performed with a fixed number of generated charges and varying the overflow electrode's voltage are represented. The overflow activation threshold is around 0-0.5 V[5].

[5]That's the reason why 0.5 V has been chosen as value for the overflow gates' voltage in the simulation reported in section 7.2.

7.4 Collection error

The floating diffusion region has a given charge capacity depending on its dimensions and on the reset voltage, which limits the charge than can be collected there. The overflow gate has to be regulated to allow in the BSI an amount of charges which can be processed also by the FD region. But with higher values of the overflow electrode's gate voltage, the collection results less effective.

The collection error is defined as:

$$E_{collection} = \frac{BSIcharge - CollectedCharge@FD}{BSIcharge} \tag{1}$$

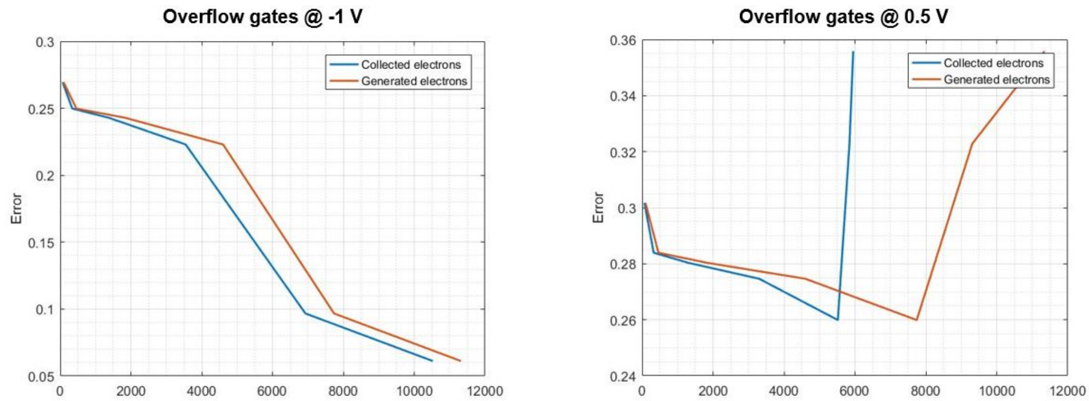

Figure 43: *FLORA with pinned diode: collection error*

The charge in the BSI is obtained as the difference between the back charge and the charge going to the overflow in the moment of the charge generation. Moreover this is always done with respect to a reference simulation where no charge is collected, for each situations with different voltage levels.

In figure 43 two extreme cases of the entity of overflow gates' voltage are represented. In particular the collection error is shown.
In the first one, when the overflow gates are at -1 V, the error is really low, but, since the side bump is quite pronounced, the charge allowed in the BSI is too much, it will saturate the FD when transferred there. However, in this case, the error that I get for the charge collection is really low, about around 5%.

Conversely, in the second case, when the overflow gates are at 0.5 V, there is the right amount of charge in the BSI region, but not all that charge is collected at the FD (the error is around 30%).
Maybe this happens because, since the side bump is very soft, when charges start to be many, they are pushed from the BSI to the overflow electrode when the transfer gates go to -3 V in order to isolate the FD region.

Actually, if it is so, you are still able to collect these charges by integrating the current through the overflow electrode. In the plots of the figure 43 this possibility is not considered.

8 Conclusions

The operation of the sensor is as desired.
Nevertheless the performances can still be improved much. Some of the possible subjects which can be further developed are:

- Finding the best compromise for the overflow gate electrode; verifying if charges flow through the overflow electrode either during charge transfer or during the isolation of the FD region;
- Changing the dimensions of the floating diffusion region in order to allow it to host the optimal amount of charges (but remembering that the smaller the capacitance of the region, the more sensitive the measurement of the collected charge);
- Studying the behavior of the sensor when changing the pinned layer voltage;
- Developing the J-FET stage for charge transfer possible, in order to make the transfer happen more deeply in the structure and avoid electrons trapped on the oxide surface (few hints in section 4.3).

This is just the beginning of the first phase of the FLORA project. A lot of work is still needed.

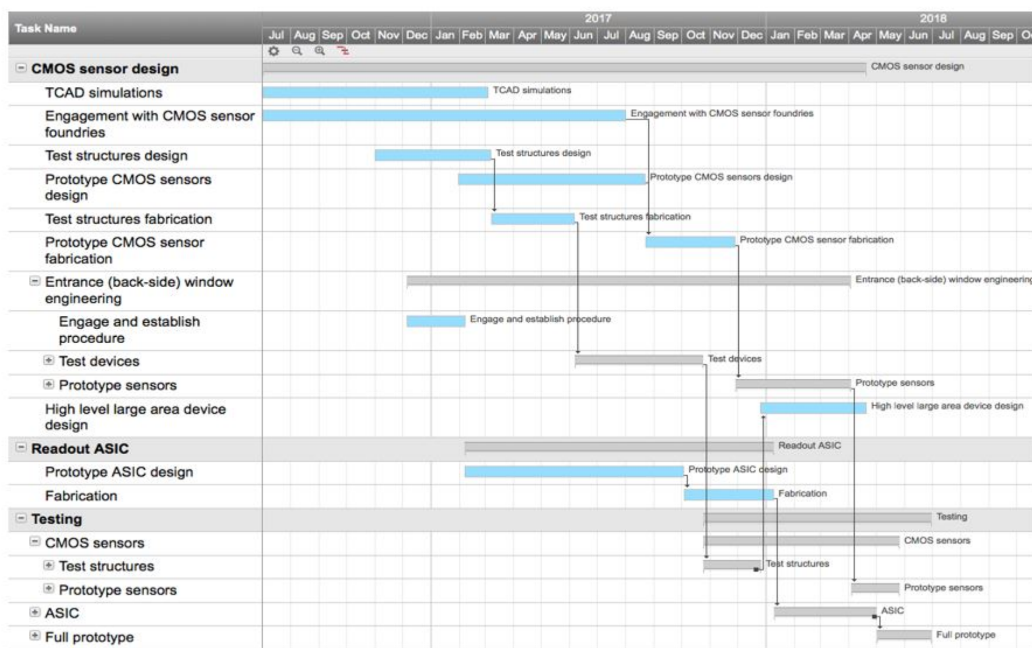

Figure 44: *Gantt diagram of the whole FLORA project*

I hope to have provided effective guidelines for the fabrication of the FLORA pixel and important hints for its further development with my 2-months work at Fermilab.

Looking forward for the realization and testing of the sensor.

Alessio Durante
Fermilab, 09/29/2017

References

[Per-Olov Petterson, 2017] Flora Pixel Design (TCAD), *Report 1 2017/06/23*.

[Carini Gabriella, 2017] Detector challenges for LCLS-II FLORA: LCLS/SLAC and Fermilab collaboration, *2017/06/20 Fermilab seminar*.

[Carini Gabriella, Deptuch Grzegorz, Fahim Farah, 2017] FLORA: A 3D-Integrated CMOS Detector for Imaging Experiments at LCLS-II, *SLAC National Accelerator Laboratory, Fermilab*.

[Pelamatti Alice, 2015] Estimation and modeling of key design parameters of pinned photodiode CMOS image sensors for high temporal resolution applications, *PhD thesis, Toulouse University*.

[Silvaco, 2017] ATHENA process simulation, *User Manual*.

[Silvaco, 2017] ATLAS device simulation, *User Manual*.

[S. M. Sze, Kwok K. Ng, 2017] Physics of Semiconductor Devices, *Wiley-Interscience, Third Edition*.